



D3.1

Producing HBI with different apparent densities as well as
evaluation of the compaction process

Partner:	TU Bergakademie Freiberg (TU BAF), ITUN, Germany
Authors:	Dr. Franz Fehse Dr. Volker Herdegen
Version:	2.0
Date:	27.06.2025



Project details

Project Title	Reoxidation behaviour and stability of direct reduced and hot briquetted iron with variable iron and carbon content to promote safe handling and transport for a future decarbonised steel production
Project Acronym	HBI C-Flex
Grant Agreement No.	101112479
Project Start Date	01.07.2023
Project End Date	31.12.2026
Duration	42 months

Document details

WP:	3
WP Leader:	AMMR
WP Title:	Experimental ore reduction, hot briquetting and HBI reoxidation studies
Task:	3.3
Task Leader:	TU BAF
Task Title:	DRI briquetting campaigns
Deliverable No.	3.1
Deliverable Title	Producing HBI with different apparent densities as well as evaluation of the compaction process
Dissemination level	PU
Written by	Dr. Franz Fehse, Dr. Volker Herdegen
Contributing beneficiary(ies)	
Approved by	Lukas Schmidt
Status	Version 2.0
Date	27.06.2025



Document history

Vers.	DATE	AUTHOR / REVIEWER	NOTES
0.1	24.01.25	Fehse, Herdegen	Preparation of initial version
0.2	28.01.25	Lukas Schmidt	Review
1.0	28.01.25	Fehse	Revision
2.0	27.06.25	Fehse	Addition of whiskers for standard deviation resp. maximum minimum measurement Standardisation of nomenclature

Disclaimer

This document is the property of the **HBI C-Flex** consortium.

This document may not be copied, reproduced, or modified in the whole or in the part for any purpose without written permission from the **HBI C-Flex** coordinator with acceptance of the project consortium.

Funded by the European Union. Views and opinions expressed are however those of the author(s) only and do not necessarily reflect those of the European Union or European Research Executive Agency (REA). Neither the European Union nor the granting authority can be held responsible for them.

This project has received funding from the Research Fund for Coal and Steel under grant agreement No 101112479.



Table of Content

Abstract.....	7
1 Introduction.....	8
2 Material.....	9
3 Methods.....	9
3.1 Experimental setup and procedure.....	9
3.2 Experimental programme	11
3.3 Parameters of evaluation.....	11
3.3.1 <i>Quality parameters of the briquettes</i>	11
3.3.2 <i>Characteristic values of the compaction behaviour</i>	13
4 Results.....	15
4.1 Influence of the parameter variation on the briquette quality	15
4.2 Description of the compaction behaviour	18
Conclusion	20
References.....	21



List of Figures

Figure 1: Experimental setup for hot briquetting at TU BAF.....	9
Figure 2: Schematic process workflow for HBI production in laboratory scale at TU BAF	10
Figure 3: Scheme of the abrasion drum at TU BAF	12
Figure 4: Force-displacement diagram for a briquetting trial (in principle) according to [1]...	13
Figure 5: Exemplary pressure-displacement diagram for the briquetting of DRI ($p = 200 \text{ MPa}$, $\vartheta_p = 800 \text{ °C}$, $t_p = 3$).....	14
Figure 6: HBI produced at different compression pressures and compression temperatures from DRI pellets from CRM.....	16
Figure 7: Relative apparent density (mean value and standard deviation) and compressive strength (mean value and minimum/maximum value) of the briquettes (left) and abrasion resistance of the briquettes (right) at different compression temperatures and compression pressures.....	16
Figure 8: Re-expansion of the briquettes and compression ratio (left) and energy of compaction (right) at different compression temperatures and compression pressures	18



Abbreviations and acronyms

Abbreviations

DRI	Direct reduced iron
HBI	Hot briquetted iron
ITUN	Institute of Thermal, Environmental and Resources' Process Engineering, TU BAF
TU BAF	TU Bergakademie Freiberg
XRD	X-ray defraction

Symbols

d	Diameter, particle size	mm
E_{EC}	Elastic energy of compaction	kNm
E_{TC}	Total energy of compaction	kNm
ε	Re-expansion of the briquette	%
F	Force	N
Fe_{met}	Metallic iron content	%
FeO	Ferrous oxide (wüstite) content	%
Fe_2O_3	Ferric oxide (haematite) content	%
Fe_3O_4	Black iron oxide (magnetite) content	%
h	Height	mm
K	Compression ratio	-
m	Mass	g
n	Number of revolutions	-
p	Pressure	MPa
R^2	Goodness of fit	
$R w_S (n)$	Abrasion resistance: residue on the screen with the width w_S after n	%
ρ	Density	g/cm ³
s	Displacement	mm
σ_P	Compressive strength	MPa
t	Time	s
ϑ	Temperature	°C
w_S	Width of the sieve	mm

Frequently used indices

app	apparent
B	briquette
max	maximum
p	compression, pressure
rel	relative



Abstract

This report summarises the investigations into HBI production in laboratory scale regarding the influence of compression pressure and compression temperature on apparent density, mechanical strength and the compaction process from DRI pellets supplied by consortium partners.



1 Introduction

On the basis of systematic laboratory tests in task 3.2, the briquetting behaviour of DRI pellets is systematically investigated. For this purpose, our project partners ArcelorMittal Maizières Research, CRM and Tata Steel provide us with DRI samples reduced at their facilities.

The main objectives are

- the production of briquettes with different apparent densities by varying the compression pressure¹ and compression temperature during HBI production and
- the description of the dependencies of the apparent density, mechanical strength and compaction behaviour on the compression pressure and compression temperature.

¹ Compression and compaction are often used synonymous in literature for densification of solids (pharmacy, process engineering etc.). To guard against misunderstandings, a definition by US Pharmacopoeia for tablet progression may be used:

Compression: Reduction of bulk volume by removal of gaseous phase by external force,

Consolidation: Increase in mechanical strength by particle-particle interactions,

Compaction: Compression and consolidation by application of external force.



2 Material

For the investigations presented in this report, a first DRI sample from CRM facility HUGE from reduction campaigns with hydrogen was used. Optically identified foreign particles were removed from the material manually. An abstract from the XRD analysis shows the following components:

- | | | | |
|------------------------------------|------------|------------------------------------|-----------|
| - Fe _{met} : | 90.5 wt.-% | - Fe ₂ O ₃ : | 2.0 wt.-% |
| - Fe ₃ O ₄ : | 2.4 wt.-% | - FeO: | 4.0 wt.-% |

3 Methods

This chapter gives an overview of the used experimental setup and the testing procedure, the number of trials as well as the evaluation parameters.

3.1 Experimental setup and procedure

As one result of work package 2, a new glove box for the DRI handling under inert conditions was erected and integrated into the consisting lab-scale facility for hot briquetting at TU BAF. The setup is shown in Figure 1.

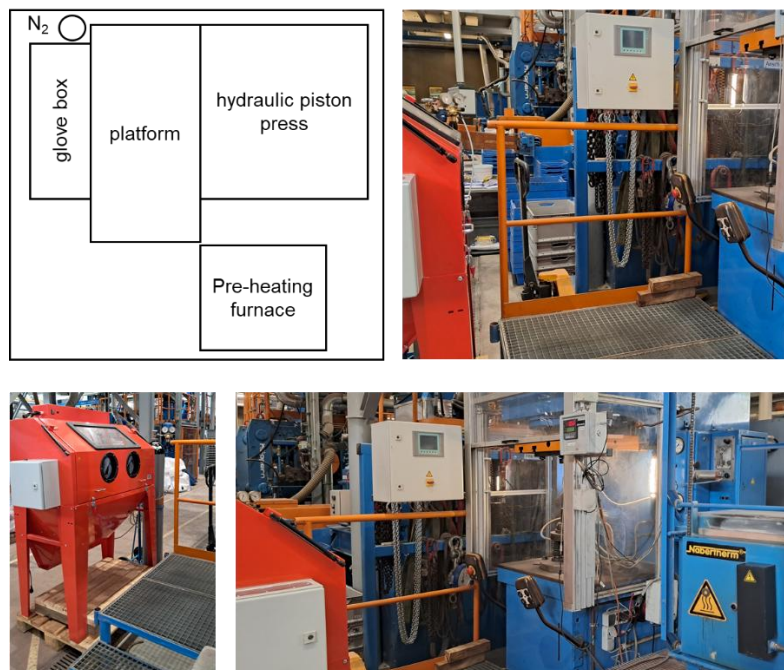


Figure 1: Experimental setup for hot briquetting at TU BAF



It consists of the previously mentioned glove box for the DRI handling, which can be rendered inert with nitrogen, the pre-heating furnace and the hydraulic piston press with a cylindrical press mould of 50 mm diameter. For the furnace (Naberterm) an inert gas purging was provided and the piston press (Wema Zeulenroda, maximum pressing force 2500 kN, compaction speed ≈ 10 mm/s) was equipped with an inert gas lance to purge the cooled press mould.

The schematic process workflow is utilised as shown in Figure 2, when a new sample of HBI should be produced.

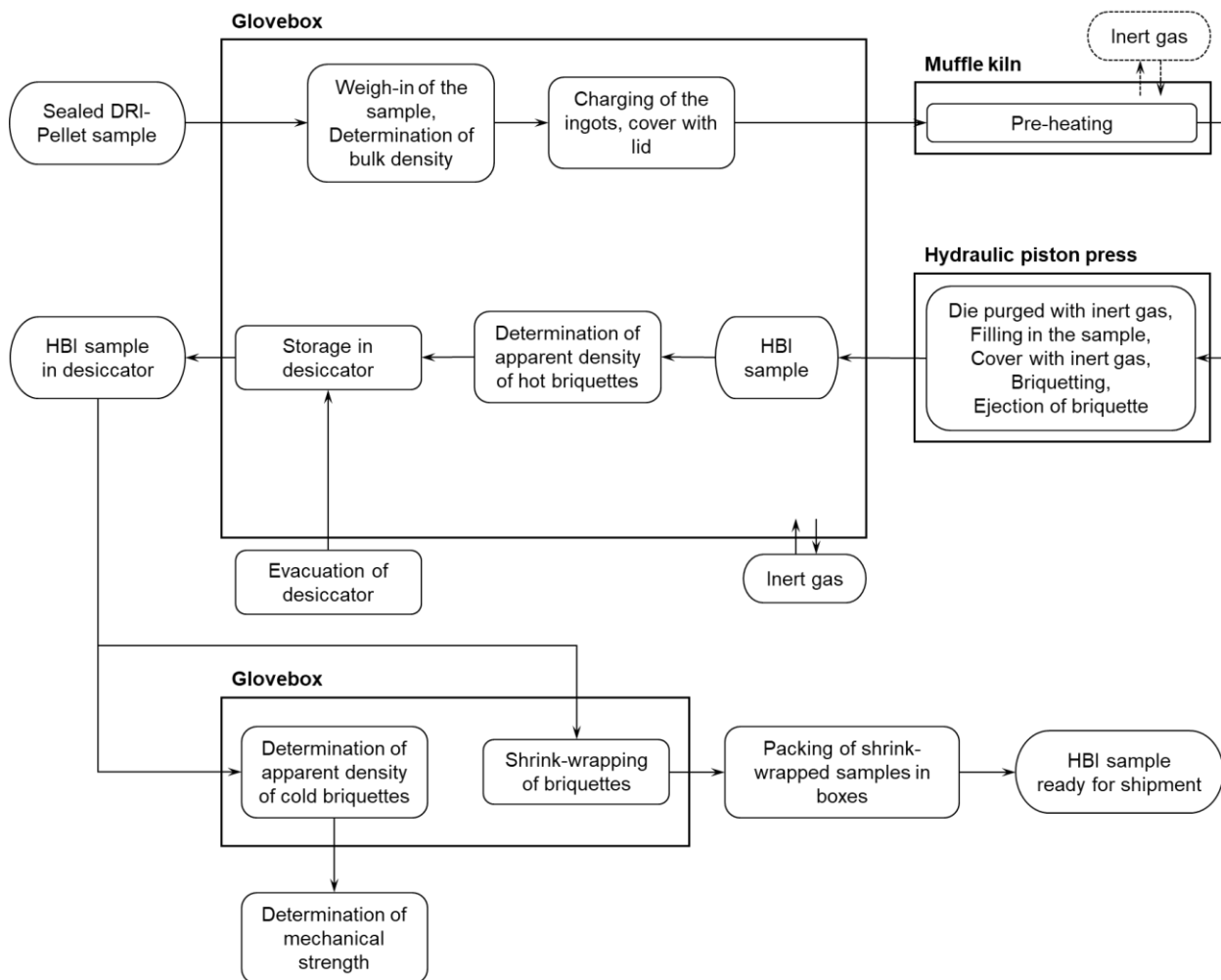


Figure 2: Schematic process workflow for HBI production in laboratory scale at TU BAF

The sealed DRI sample from our partner is put into the glovebox in nitrogen atmosphere. It is opened subsequently and a small sample portion is taken for characterisation. Afterwards, the samples for hot briquetting are weighed in and the bulk density is determined before filling the sample in the ingots. The mass of the sample taken remains constant at 150 g for each



briquette. The filled ingots are covered with a lid and are then transferred into the muffle furnace (with nitrogen atmosphere). The furnace is previously heated to the chosen briquetting temperature. After one hour the sample reached the favourable temperature. Before taking the sample out of the furnace, the press mould at the hydraulic piston press is purged with nitrogen. Afterwards, the DRI pellets from the ingots are filled into the press mould and the DRI is once more covered with inert gas. Then, the briquetting process starts – the piston moves down into the mould and agglomerates the DRI sample at the chosen compression pressure. The time at maximum compression pressure remains constant for all trials at 3 s. When the briquette is ejected from the press, the produced HBI is transferred directly into the glove box. Weight and dimensions (height, diameter) of the briquette are recorded directly and it is stored in a previously evacuated desiccator. This process is at least repeated five times for each set operating conditions.

After one day the weight and dimensions of the briquettes are measured once more and the mechanical strength in terms of abrasion resistance and compressive strength is determined. If required, a sample is shrink-wrapped, put in a sealed box and sent to our project partner Montanuniversität Leoben for re-oxidation trials.

3.2 Experimental programme

In systematic laboratory experiments, the influence of compression pressure and compression temperature on the apparent density and the mechanical strength of the briquettes are investigated. The compression pressure was varied stepwise between 150 MPa, 200 MPa and 300 MPa. The compression temperature was varied stepwise between 600 °C, 800 °C and 900 °C.

3.3 Parameters of evaluation

3.3.1 Quality parameters of the briquettes

Apparent density

The apparent density of the briquette is calculated by the mass and volume of the briquette according to equation 1. The mass is determined by weighing and the volume is determined by measuring the diameter and the height of the briquette. The mean of the apparent density is calculated from the quintuplicate.

$$\rho_{\text{app}} = \frac{4 m_B}{\pi d_B^2 h_B} \quad [\rho_{\text{app}}] = \frac{\text{g}}{\text{cm}^3} \quad (1)$$



For an easier comparison of the data, the relative apparent density was defined as the ratio of measured apparent density and the current target value of the HBI apparent density of 5 g/cm³:

$$\rho_{app,rel} = \frac{\rho_{app}}{5 \text{ g/cm}^3} \quad (2)$$

In the chart, the mean of the relative apparent density of five measurements is given as well as the standard deviation using whiskers.

Compressive strength

For the determination of the compressive strength, the briquette is put on a universal testing machine (Shimadzu, Type UHA 500 kN) between two plane-parallel pistons ($d = 30 \text{ mm}$) and loaded until breakage. The maximum pressure is taken as the value for the maximum briquette compressive strength σ_{pB} in MPa. Unless otherwise stated, the compressive strength is determined on two briquettes and the mean is calculated.

To simplify comparability, the relative compressive strength ($\sigma_{pB,rel}$) is determined and specified from the compressive strengths σ_{pB} determined in relation to the maximum determinable compressive strength $\sigma_{pB,max,UHA500kN}$ at the used testing machine (707.8 MPa):

$$\sigma_{pB,rel} = \frac{\sigma_{pB}}{\sigma_{pB,max,UHA500kN}} \quad (3)$$

In the chart, the mean of the relative compressive strength of two measurements is given. Minimum and maximum measurements are indicated with whiskers.

Abrasion resistance

The abrasion resistance is determined in a cylindrical drum with a diameter and length of 500 mm according to Figure 3 and a rotational speed of 25 rpm.

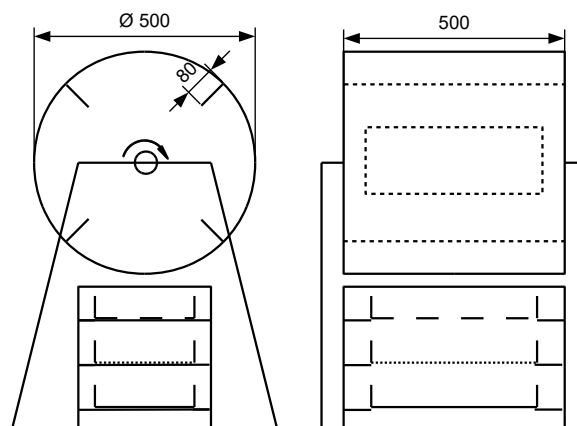


Figure 3: Scheme of the abrasion drum at TU BAF

After 100, 300, 650 and 1000 revolutions (n) the residue of the three tested briquettes on the 30 mm and 10 mm screen is determined. The abrasion resistance is calculated as the residue



mass on the relevant sieve referred to the sample mass before the test. That means exemplarily for the abrasion resistance after 100 revolutions on the 30 mm sieve:

$$R30(100) = \frac{m_{30}}{m_{tot}} \cdot 100 \% \quad [R30(100)] = \% \quad (4)$$

3.3.2 Characteristic values of the compaction behaviour

Force-displacement curve and energy of compaction

The agglomeration in a piston press is one form of press agglomeration. The particles are brought together by the external force of the hydraulic press. To describe this process of agglomeration, a force-displacement diagram or, respectively, a pressure-displacement-diagram is recorded for each briquetting trail as shown in the following Figure 4. Pressure-displacement data pairs were recorded with 200 Hz at the used hydraulic piston press whereof force-displacement data can be easily calculated. The information, that can be taken from this chart as shown in Figure 4, is explained below.

When the piston moves down into the mould and starts to contact the heated DRI, the pressure rises with increasing compaction of the material until it reaches the maximum force F_{max} (depending on the set compression pressure) at the maximum displacement of the piston s_{max} . This process is described by the compaction curve $F_C(s)$. When the piston is retracted, the force does not directly fall to zero but decreases with the returning piston due to the elastic behaviour of the agglomerate resulting in the re-expansion of the briquette in height. This process is described by the re-expansion curve $F_R(s)$.

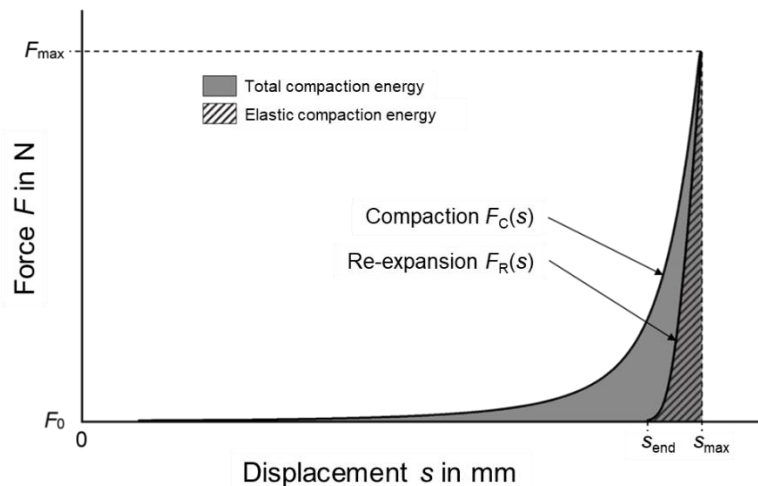


Figure 4: Force-displacement diagram for a briquetting trial (in principle) according to [1]

The total energy of compaction E_{TC} is represented by the area under the compaction curve. The energy, which is released from the briquette during re-expansion, is called elastic energy of compaction E_{EC} and is represented by the area under the re-expansion curve (hatched area).



In the here discussed briquetting tests, pressure-displacement or, respectively, force-displacement diagrams as shown in Figure 5 were recorded.

From the recorded data maximum pressure, maximum force and maximum displacement of the piston were determined. The total compaction energy, which is the area under both force-displacement curves, was calculated using the difference method. In the chart, the mean of the total compaction energy of six measurements is given as well as the standard deviation using whiskers. The elastic energy of compaction E_{EC} is not calculated at this point.

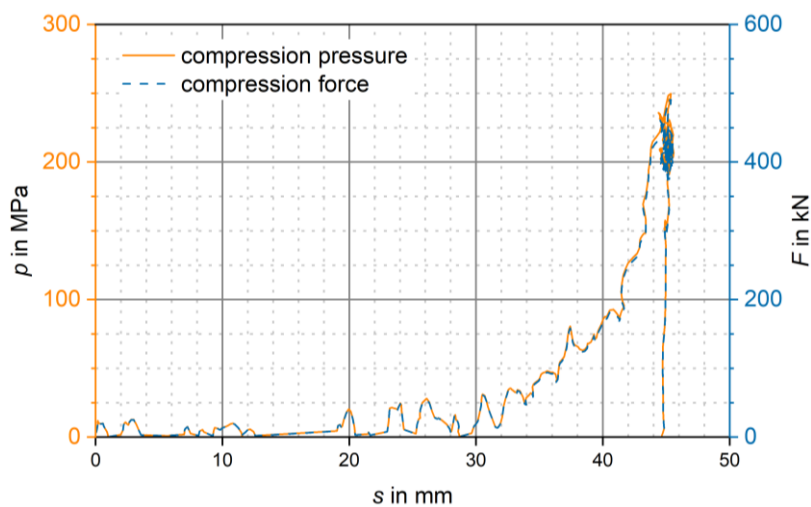


Figure 5: Exemplary pressure-displacement diagram for the briquetting of DRI
($p = 200$ MPa, $\vartheta_P = 800$ °C, $t_P = 3$)

Elastic re-expansion

In combination with data of briquette quality, the elastic re-expansion of the briquettes in % can be calculated from the compaction curve:

The maximum displacement of the piston in the empty mould was recorded before each trial. The difference between the maximum displacement of the piston, when the press channel is empty ($s_{\max, \text{empty}}$), and the maximum displacement of the piston, when the press channel is filled (s_{\max}), is the briquette height under pressure ($h_{B,p}$):

$$h_{B,p} = s_{\max, \text{empty}} - s_{\max} \quad [h_{B,p}] = \text{mm} \quad (5)$$

The elastic re-expansion ε is calculated as the quotient of the change in height (under pressure and after ejection) and height under pressure:

$$\varepsilon = \frac{h_{B,p} - h_{B,e}}{h_{B,p}} \cdot 100 \% \quad [\varepsilon] = \% \quad (6)$$

In the chart, the mean of the elastic re-expansion of six measurements is given as well as the standard deviation using whiskers.



Compression ratio

Before filling the ingots, the bulk density of the sample taken is determined in a cylinder of 50 mm diameter by measuring the height of the bulk ($h_{bulk,sample}$) and the sample mass. Considering the height of the briquette under pressure, the compression ratio (K) is calculated as follows:

$$K = \frac{h_{bulk,sample}}{h_{B,p}} \quad (7)$$

In the chart, the mean of the compression ratio of six measurements is given as well as the standard deviation using whiskers.

4 Results

In this chapter the results of the briquetting trials for the DRI pellets from CRM are presented and discussed.

4.1 Influence of the parameter variation on the briquette quality

The briquetting behaviour of the DRI pellets was investigated at three different compression pressures (150 MPa, 200 MPa and 300 MPa). For each compression pressure the compression temperature was varied in three stages (600 °C, 800 °C and 900 °C).

The photos in Figure 6 give an optical impression of the produced HBI at the different parameter sets. Especially at the lower compression pressure, the grain boundaries of the single DRI pellets are still visible in the briquette. Nevertheless, the briquettes offer smooth surfaces and clear edges without chips.

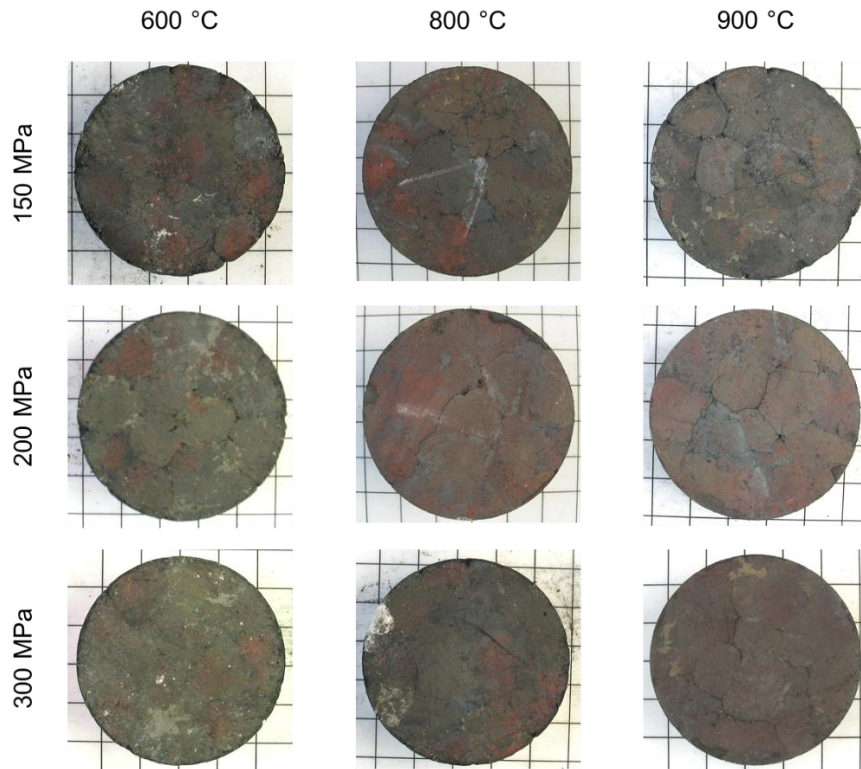


Figure 6: HBI produced at different compression pressures and compression temperatures from DRI pellets from CRM

In Figure 7 the relative apparent density, the relative compressive strength and the abrasion resistance of the briquettes are shown for the set compression pressures and temperatures.

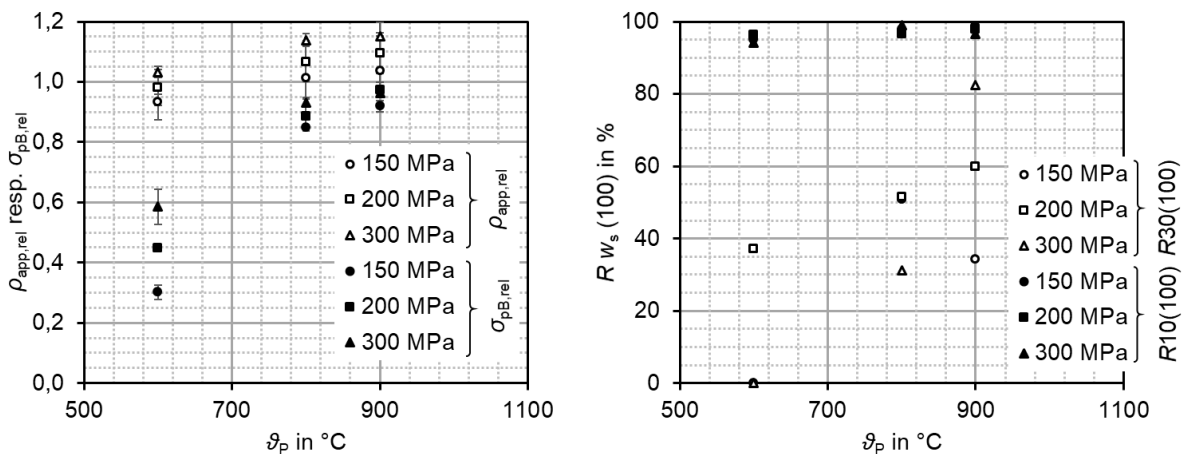


Figure 7: Relative apparent density (mean value and standard deviation) and compressive strength (mean value and minimum/maximum value) of the briquettes (left) and abrasion resistance of the briquettes (right) at different compression temperatures and compression pressures



At the lowest compression pressure of 150 MPa in combination with the lowest compression temperature (600 °C) the HBI offers the lowest relative density and compressive strength. Nevertheless, the relative density of the briquettes of 0.93 is already close to the target value of 1. After 100 revolutions in the drum the briquettes are broken. The residue on the 10 mm sieve amounts to 95 %. This means 95 % of the pieces of the briquettes are bigger than 10 mm.

An increase in compression pressure at constant temperature is followed by slightly higher apparent densities. At a compression pressure of 300 MPa at 600 °C, the apparent density exceeds the target value of 1. The compressive strength also increases with a higher compression pressure. A doubling of the compression pressure nearly leads to a doubling in compressive strength for the investigated operating conditions. Regarding the abrasion resistance R30(100), an increase in compaction pressure from 150 MPa to 200 MPa results in a higher abrasion resistance.

When the compression temperature rises to 800 °C, the apparent density increases. This increase in compression temperature shows a much higher impact in comparison to the increase in compression pressure. The compressive strength of the briquettes is on a significantly higher level when the temperature is set to 800 °C. In contrast to the apparent density, the influence of the compression pressure on the compressive strength decreases at the higher compression temperature. At 800 °C, the briquettes also offer a higher abrasion resistance.

An increase in compression temperature to 900 °C results in briquettes with the highest quality. The effect on the apparent density may not be significant, but a slight increase of the mean relative apparent density is noticeable. The higher temperature leads to a further decrease in influence of the briquetting pressure on compressive strength. Due to the increase in temperature, the abrasion resistance improves considerably.

A multiple regression of relative apparent density and relative compressive strength as a function of compression pressure and compression temperature made clear that the relationship of both evaluation parameters with the two factors can be described satisfactorily by a linear model:

$$\rho_{\text{app,rel}} = 0.5954 + 0.0007 p + 0.0004 \vartheta_p \quad (8)$$

$$R_{\text{korr}}^2 = 0.9647$$

$$\sigma_{\text{pB,rel}} = -0.8002 + 0.0009 p + 0.0018 \vartheta_p \quad (9)$$

$$R_{\text{korr}}^2 = 0.8916$$



4.2 Description of the compaction behaviour

In a further step, the recorded force-displacement data or, respectively, pressure-displacement data for each briquette in each trial was analysed according to the procedure described in section 3.3.2. For each trial the means for each of the characteristic values were calculated from the six single values. Figure 8 shows the means of elastic re-expansion of the briquettes, the compression ratio of the briquettes and the energy of compaction as a function of compression pressure and compression temperature.

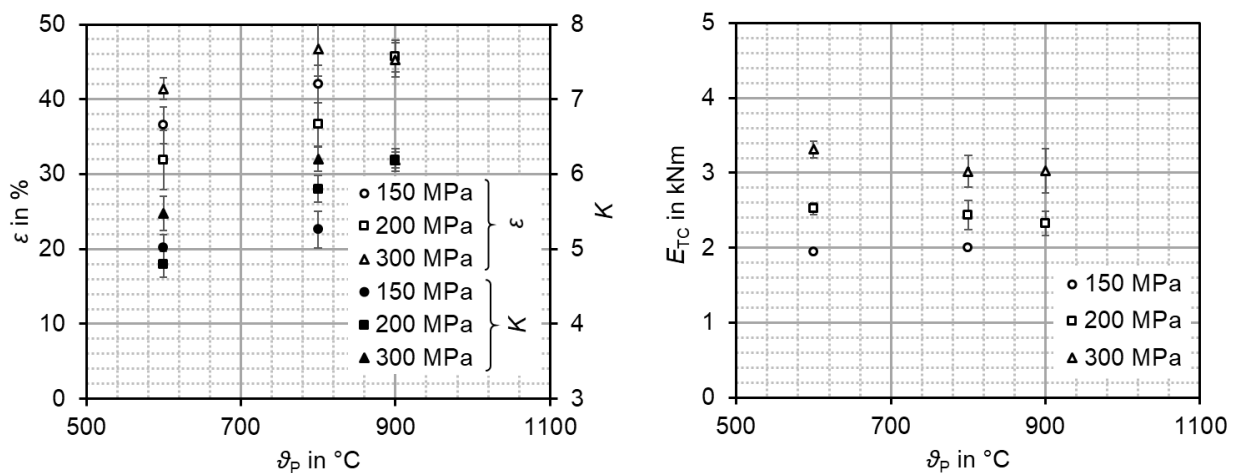


Figure 8: Re-expansion of the briquettes and compression ratio (left) and energy of compaction (right) at different compression temperatures and compression pressures (please note the unanalysable data at 150 MPa/ 900 $^{\circ}\text{C}$ for the energy of compaction)

By using higher compression pressures, the energy of compaction increases. At a compression temperature of 600 $^{\circ}\text{C}$, the compression pressure shows the highest influence on the energy of compaction. When a compression temperature of 800 $^{\circ}\text{C}$ is chosen, the influence of the pressure slightly decreases. Due to the higher plasticity, the densification becomes easier and, especially, at a compression pressure of 300 MPa, the necessary energy of compaction decreases in comparison to the compaction energy at lower temperatures.

Regarding the re-expansion of the briquettes, a higher compression pressure leads to a higher re-expansion of the briquettes, generally. At 900 $^{\circ}\text{C}$ the influence of the pressure decreases leading to a nearly constant re-expansion of the briquettes. Due to the higher plasticity of the DRI pellets at the higher temperature and the stronger solid bridges building between the particles, a stronger agglomerate with higher plastic deformation and lower re-expansion can be produced.



As a last characteristic value, the compression rate is determined. In general, higher pressure and higher temperature should lead to a higher compression rate. This trend can also be noticed in the data of these investigations. Additionally, if the compaction rate remains constant for increasing pressure or temperature this might be a sign for a stagnant densification. Regarding the compression rate at 300 MPa with increasing temperature from 800 °C to 900 °C it nearly remains constant. Taking the lower re-expansion of the briquette into account, the apparent density remains at a high level and the briquettes offer the strongest mechanical strength.



Conclusion

In this report, the production of HBI with different apparent densities as well as mechanical strength and characteristic values of the compaction process were presented and discussed. DRI from our project partner CRM was used for the investigation, which was produced in reduction campaigns with H₂ at their HUGE facility. The results may be summarised as follows:

- The production of DRI with different apparent densities is possible by adaption of the compression pressure and the compression temperature. Higher pressure as well as higher temperature leads to higher apparent density as expected.
- The compressive strength of the briquettes is generally on a high level. Generally, a higher compression temperature shows a positive influence on the compressive strength. With increasing compression temperature, the influence of compression pressure on the compressive strength decreases.
- In the investigated range of the set operating conditions, the apparent density and the compressive strength can be described as a function of the compression pressure and the compression temperature using linear equations.
- The compaction process was described with the energy of compaction, the re-expansion of the briquettes and the compaction rate. With increasing temperature, the energy of compaction decreases, especially, in combination with a high briquetting pressure of 300 MPa due to the higher plasticity of the DRI and the stronger solid bridges formed between the pellets in the briquette.

In further experiments, the influence of material composition (e. g. carbon content, metallic iron content, total iron content) on HBI quality will be systematically investigated to develop a generalised model for the compaction process and for the prediction of the HBI quality.



References

- [1] St. Höntsch, F. Fehse, H.-W. Schröder, V. Herdegen, A. S. Braeuer, Influence of comminution and briquetting parameters on the agglomeration behaviour of wheat straw. Biomass and Bioenergy 182 (2024), article no. 107077